chemistry proceedings

MDPI

Proceedings Paper

N,N-dimethyl-4-amino-2,1,3-benzothiadiazole: Synthesis and Luminescent Solvatochromism †

Valentina Ferraro *, Matteo Girotto and Marco Bortoluzzi

Dipartimento di Scienze Molecolari e Nanosistemi, Università Ca' Foscari Venezia, Via Torino 155, 30170 Mestre, VE, Italy; 857524@stud.unive.it (M.G.); markos@unive.it (M.B.)

* Correspondence: valentina.ferraro@unive.it; Tel.: +39-041-234-8651

† Presented at the 25th International Electronic Conference on Synthetic Organic Chemistry, 15–30 November 2021; Available online: https://ecsoc-25.sciforum.net/.

Abstract: *N,N*-dimethyl-4-amino-2,1,3-benzothiadiazole (BTD^{NMe2}) was synthesized from the commercially available 2,1,3-benzothiadiazole (BTD) by nitration in sulfonitric mixture, followed by reduction of the nitro-group and subsequent methylation with iodomethane. BTD^{NMe2} was fully characterized by means of nuclear magnetic resonance (NMR) and infrared spectroscopy. Solutions of BTD^{NMe2} in common organic solvents revealed to be appreciably luminescent in the visible range. The electronic transitions related to the absorption and emission properties were associated to the HOMO-LUMO energy gap by means of electrochemical measurements and DFT calculations. Finally, BTD^{NMe2} was successfully used for the preparation of luminescent doped poly(methyl methacrylate) samples.

Keywords: *N,N*-dimethyl-4-amino-2,1,3-benzothiadiazole; fluorescence; solvatochromism; 2,1,3-benzothiadiazole

Citation: Ferraro, V.; Girotto, M.; Bortoluzzi, M. *N,N*-dimethyl-4-amino-2,1,3-benzothiadiazole: Synthesis and Luminescent Solvatochromism. *Chem. Proc.* **2021**, *3*, x. https://doi.org/10.3390/xxxxx

Academic Editor: Julio A. Seijas

Published: 15 November 2021

1. Introduction

2,1,3-benzothiadiazole (BTD) is a π-extended heteroarene that was used for a wide range of applications such as herbicide, fungicide and antibacterial agent [1]. However, it is also applied for the preparation of luminescent materials owing to the combination of strong withdrawing ability and behaviour as fluorophore [2]. Intermolecular interactions such as heteroatom contacts and π–π stacking determine well-ordered structures [3]. Over the last decades, polymers [4] and liquid crystals [5] containing the BTD fragment were successfully exploited for advances applications [6] such as organic light-emitting diodes (OLEDs) [7,8], dyes [9–14], solar and photovoltaic cells [15–18]. 2,1,3-benzothiadiazole-based compounds were also exploited as fluorescent probes for the bioimaging in live cells [19–21] or as fluorescent polymeric thermometers for the determination of intercellular temperature [22,23]. Moreover, poly(benzothiadiazoles) were used as heterogeneous photocatalysts able to promote various organic photoredox reactions under visible-light irradiation [24,25].

Despite the fact that 4-amino-2,1,3-benzothiadiazole was deeply investigated both as free compound [26] and as possible ligand [27–33] for the preparation of transition metal complexes, *N,N*-dimethyl-4-amino-2,1,3-benzothiadiazole (BTD^{NMe2}) was much less studied. The only preparation reported in literature dates back to 1976 [34], but the compound was only poorly characterized. Herein, we report an alternative synthesis and the characterization of BTD^{NMe2}, with particular interest towards the photophysical properties of the compound. The possible application of BTD^{NMe2} as dopant for polymeric materials was also explored.

2. Materials and Methods

Commercial solvents (Merck) were purified following literature methods [35]. 2,1,3-benzothiadiazole and the other reagents were Aldrich products, used as received. Poly(methyl methacrylate) (PMMA, M_w = 86,000 g mol^{-1}) was a TCI Chemicals product. 4-nitro-2,1,3-benzothiadiazole (BTD^{NO2}) was synthesized by modifying a reported procedure [36]. 24 mL of H_2SO_4 98% and 8 mL HNO_3 70% were mixed in a flask and frozen with a nitrogen bath. 2,1,3-benzothiadiazole (2.000 g, 14.7 mmol) was added, then the reaction was allowed to warm up at room temperature and stirred for three hours. The reaction mixture was then cooled with an ice bath and water (15 mL) was slowly added. Subsequently, a solution containing about 18.0 g of NaOH in 40 mL of water was added within an hour. After removal of the ice bath, $NaHCO_3$ was added in small amounts until neutral pH was reached. The product was extracted with 2 × 40 mL of dichloromethane and the organic fraction was washed with water (2 × 20 mL), dried over Na_2SO_4 and evaporated under reduced pressure to afford a reddish solid. Yield: 95%. Characterization data are in agreement with those reported for the same product obtained with different synthetic routes [37]. The reduction of 4-nitro-2,1,3-benzothiadiazole (BTD^{NO2}) to afford the corresponding 4-amino-2,1,3-benzothiadiazole (BTD^{NH2}) was carried out following a reported procedure [38], with slight modifications. To a solution containing 2.000 g of BTD^{NO2} (11.4 mmol) in 50 mL of ethanol 9.208 g of $FeSO_4{\cdot}7H_2O$ (34.2 mmol), 4.878 g of ammonium chloride (91.2 mmol), 9 mL of water and 2.243 g of zinc dust (34.2 mmol) were added under vigorous stirring. The mixture was heated at 50 °C for three hours and, after cooling at room temperature, it was cleared by filtration on celite. The solid was washed with 3 × 10 mL of ethanol. The solution thus obtained was evaporated under reduced pressure. The crude product was dissolved in 40 mL of ethyl acetate and 30 mL of a 25% aqueous solution of NH_4Cl were added. The organic layer was extracted and washed with water (2 × 20 mL) and with 30 mL of a saturated aqueous solution of $NaHCO_3$. The organic fraction was then dried over Na_2SO_4 and concentrated under reduced pressure. The product was precipitated with isohexane and dried in vacuo. Yield: 45%. Characterization data are in agreement with the ones reported for the same product prepared with different synthetic routes [28].

Elemental analyses (C, H, N, S) were carried out using an Elementar Unicube microanalyzer. Infrared (IR) spectra were registered using a Perkin-Elmer SpectrumOne spectrophotometer between 4000 and 400 cm^{-1} using KBr disks. Mono- and bidimensional nuclear magnetic resonance (NMR) spectra were collected employing Bruker Avance 300 and Avance 400 instruments operating respectively at 300.13 MHz and 400.13 MHz of ^1H resonance. ^1H and ^{13}C NMR spectra are referred to the partially non-deuterated fraction of the solvent, itself referred to tetramethylsilane.

Absorption spectra were collected in the range 235–700 nm employing a Perkin-Elmer Lambda 40 spectrophotometer. Photoluminescence emission (PL) spectra were registered at room temperature using a Horiba Jobin Yvon Fluorolog-3 spectrofluorometer. A continuous wave xenon arc lamp was used as source and the excitation wavelength was selected using a double Czerny–Turner monochromator. Suitable long pass filters were placed in front of the acquisition systems. The detector was composed of a single monochromator iHR320 and a photomultiplier tube Hamamatsu R928. Fluorescence quantum yields Φ_f of $5{\cdot}10^{-5}$ M solutions were calculated using $5{\cdot}10^{-5}$ M anthracene in ethanol as standard on the basis of Equation (1) [39], where $\Phi_{f,std}$ is the quantum yield of anthracene in ethanol (0.27), F and F_{std} are respectively the areas under the fluorescence emission bands of the sample and of the standard, A and A_{std} are respectively the absorbance values of sample and standard at the excitation wavelength, n is the refractive index of the solvent used for the sample and n_{std} is the refractive index of ethanol.

$$\Phi_f = \Phi_{f,std} (F\ A_{std}\ n^2)(F_{std}\ A\ n_{std}^2)^{-1} \quad (1)$$

Electrochemical measurements were carried out on dry acetonitrile solutions of BTD^{NMe2}, containing $LiClO_4$ as supporting electrolyte and ferrocene (Fc) as internal reference. The instrument used was an eDAQ ET014-199 potentiostat, connected to eDAQ 1 mm glassy carbon disk working electrode, eDAQ 1.6 mm diameter Pt/Ti counter-electrode and a Pt wire as reference. The couple Fc/Fc^+ was used as internal standard and all the measurements were carried out at room temperature under argon atmosphere.

Computational calculations were carried out using the range-separated hybrid DFT functional ωB97X in combination with Alhrichs' def2-TZVP basis set [40–43]. The C-PCM conductor-like polarizable continuum model was added, considering acetonitrile as a continuous medium [44,45]. The TD-DFT approach was used to simulate the electronic transitions [46]. Gaussian 16 was employed as calculation software [47].

Synthesis of *N*,*N*-dimethyl-4-amino-2,1,3-benzothiadiazole, BTD^{NMe2}: The *N*-methylation of 4-amino-2,1,3-benzothiadiazole (BTD^{NH2}) was carried out by modifying a reported procedure [48]. 0.350 g of BTD^{NH2} (2.3 mmol) were dissolved in 15 mL of *N*,*N*-dimethylformamide (DMF), then 3.179 g of K_2CO_3 (23.0 mmol) and 1.4 mL of CH_3I (23.0 mmol) were added under stirring. The mixture was heated at 75 °C for twelve hours. After cooling at room temperature, 50 mL of water were added and the product was extracted with 2 × 80 mL of ethyl acetate. The organic fraction was washed with 100 mL of cold water, dried over Na_2SO_4 and evaporated under reduced pressure. The product was dissolved in 30 mL of pentane, the solution was purified by filtration and the solvent was removed under nitrogen flow to afford a red oil. Yield: 50%.

Characterization of di N,N-dimethyl-4-amino-2,1,3-benzothiadiazole

Anal. calcd for $C_8H_9N_3S$ (179.24 g mol^{-1}, %): C, 53.61; H, 5.06; N, 23.44; S, 17.89. Found (%): C, 53.40; H, 5.08; N, 23.35; S, 17.82. ^1H NMR ($CDCl_3$, 298 K) δ 7.49–7.40 (m, 2H, BTD), 6.57 (t, 1H, $^3J_{HH}$ = 5.9 Hz, BTD), 3.29 (s, 6H, Me). ^{13}C {^1H} NMR ($CDCl_3$, 298 K) δ 156.90 BTD-C_{ipso}, 149.29 BTD-C_{ipso}, 144.43 BTD-C_{ipso}, 130.73 BTD-CH, 111.13 BTD-CH, 108.85 BTD-CH, 42.59 Me. IR (KBr disk, cm^{-1}): 1587 m, 1545 s, 1494 m (aromatic ν_{C-N} and ν_{C-C}).

Synthesis of BTD^{NMe2}@PMMA: 0.250 g of PMMA were dissolved in 6 mL of dichloromethane under slow stirring, then a solution containing 0.010 g of BTD^{NMe2} in 4 mL of dichloromethane was added. The solution was transferred in a cylindrical polyethylene holder (1 cm diameter) and allowed to evaporate at room temperature. The polymeric film thus obtained was finally kept overnight under 10^{-2} torr vacuum to remove traces of solvent.

Characterization of BTD^{NMe2}@PMMA. PL (solid sample, $\lambda_{excitation}$ = 400 nm, nm): 606. PLE (solid sample, $\lambda_{emission}$ = 605 nm, nm): < 560.

3. Results and Discussion

The synthetic route here proposed for BTD^{NMe2} starts with the nitration of the 2,1,3-benzothiadiazole heterocycle, followed by reduction of the nitro group and subsequent methylation with methyl iodide, as depicted in Scheme 1. As observable from the ^1H, ^{13}C {^1H} and ^1H–^{13}C HSQC NMR reported in Figure 1, the methyl groups are associated to a singlet at 3.29 ppm (^{13}C resonance at 42.59 ppm), while the aromatic protons of the heterocycle resonate in the 7.50–6.50 range (^{13}C resonances at 130.73, 111.13 and 108.85 ppm). The signals attributable to the three *ipso*-carbons can be detected respectively at 144.43, 149.28 and 156.90 ppm.

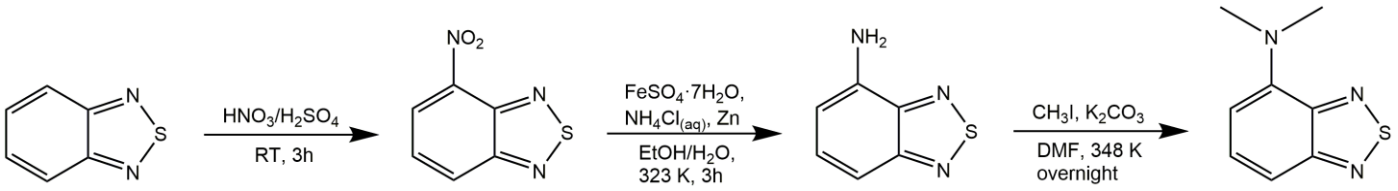

Scheme 1. Synthesis of *N*,*N*-dimethyl-4-amino-2,1,3-benzothiadiazole, BTD^{NMe2}.

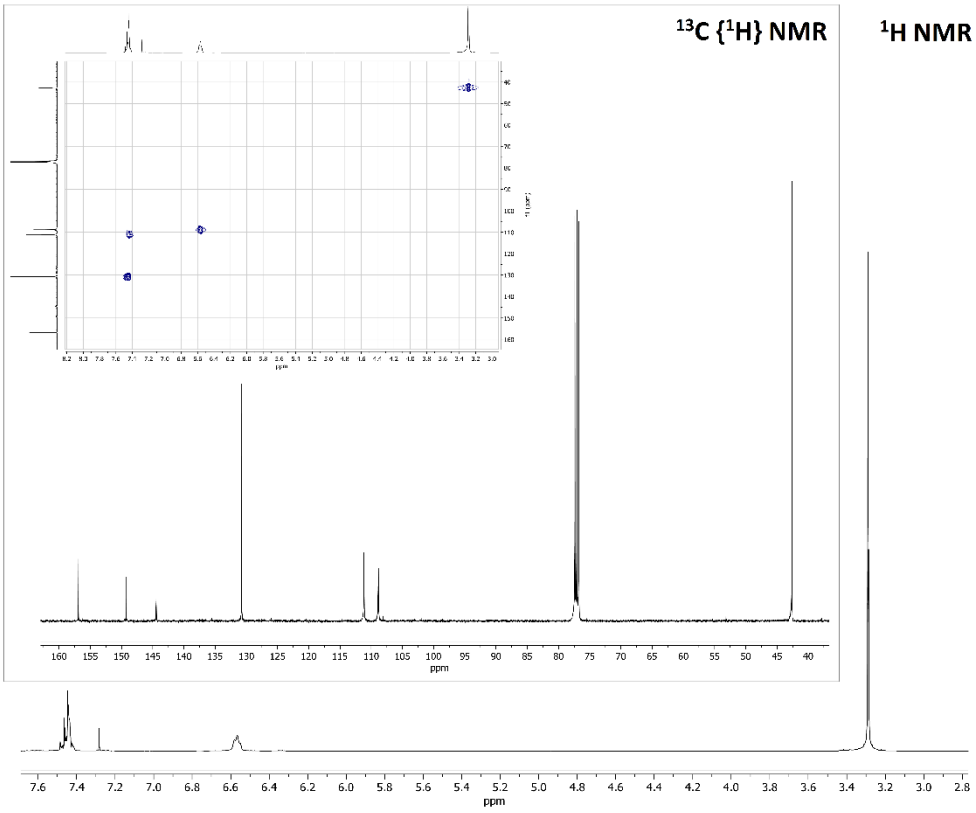

Figure 1. ^{1}H NMR spectrum of BTD^{NMe2}. Inset: ^{13}C $\{^{1}H\}$ NMR and ^{1}H-^{13}C HSQC in $CDCl_3$ at 298 K. $CDCl_3$, 298 K.

The compound was isolated as a dark red oil that exhibited intriguing luminescent properties once dissolved in common organic solvents (see Figure 2). The pure oil itself did not display appreciable emissions probably because of concentration quenching. The evident solvatochromism was investigated considering four solvents characterized by different dielectric constants ε (*n*-hexane, dichloromethane, acetone and acetonitrile). The absorption and emission spectra are shown in Figure 2. Selected properties of the solvents, including the orientation polarizability Δf (see Equation (2)), are summarized in Table 1. The table also reports absorption and emission maxima of BTD^{NMe2}, Stokes shifts $\tilde{\upsilon}_A$-$\tilde{\upsilon}_F$ and Φ_f values, calculated accordingly to Equation (1).

$$\Delta f = (\varepsilon\text{-}1)(2\varepsilon + 1)^{-1} - (n^2 - 1)(2n^2 + 1)^{-1} \quad (2)$$

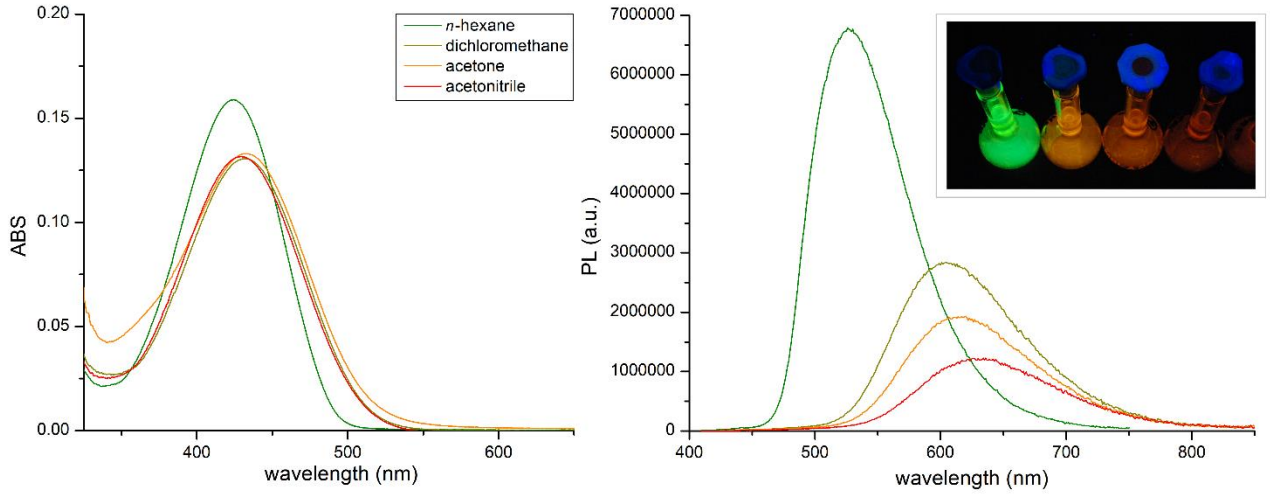

Figure 2. Absorption (**left**) and emission (**right**) spectra of $5 \cdot 10^{-5}$ M solutions of BTD^{NMe2} in different solvents recorded at room temperature. Inset: picture of the solutions under UV light ($\lambda_{excitation}$ = 365 nm).

Table 1. Fluorescence data of BTD^{NMe2} in different solvents.

Solvent	ε	n	ABS max (nm) [a]	PL max (nm) [b]	$\tilde{\upsilon}_A$-$\tilde{\upsilon}_F$ (cm^{-1})	Φ_F (%) [c]	Δf
n-hexane	1.9	1.375	424	526	4559	52	0.001
Dichloromethane	8.9	1.424	432	604	6613	41	0.217
Acetone	20.7	1.359	433	616	6872	23	0.284
Acetonitrile	37.5	1.479	430	630	7448	16	0.305

[a] 298 K. [b] $\lambda_{excitation}$ = 390 nm, 298 K. [c] Data obtained using a solution of anthracene in ethanol as standard (Φ_f = 27%) [49].

As presented in Figure 2 and Table 1, solvents characterized by higher ε values determine a bathochromic shift of the emission maxima in solution together with an increase in the Stokes shift, that varies from 4559 cm^{-1} in hexane to 7448 cm^{-1} in acetonitrile (see Table 1). The greatest variations occur on changing the solvent from hexane to dichloromethane, with a shift of the emission maximum from 526 to 604 nm and a consequent increase of the Stokes shift from 4559 cm^{-1} to 6613 cm^{-1}. The CIE 1931 chromaticity coordinates are reported in the diagram in Figure 3, where it is observable the change of emission from yellowish green to reddish orange on increasing the ε value. The colour purity of the emission of BTD^{NMe2} in hexane is 0.79, while it is almost unitary for the other solvents.

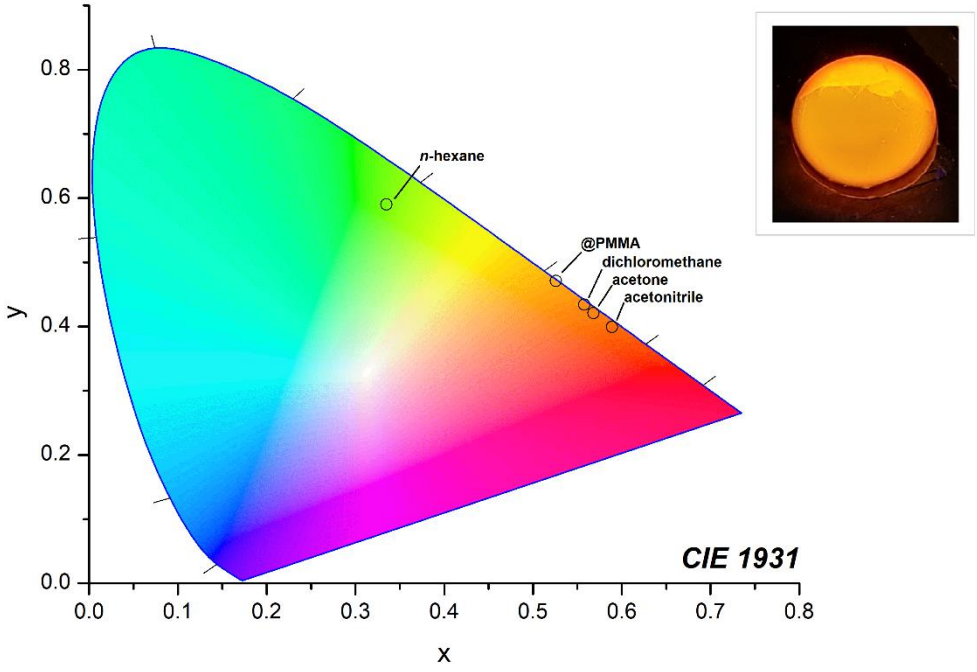

Figure 3. CIE 1931 chromaticity diagram of BTD^{NMe2} in different solvents and in PMMA (*n*-hexane: x = 0.335, y = 0.590; dichloromethane: x = 0.558, y = 0.434; acetone: x = 0.561, y = 0.421; acetonitrile: x = 0.589, y = 0.399; @PMMA: x = 0.526, y = 0.471). Inset: BTD^{NMe2}@PMMA excited at 365 nm.

The increase of dielectric constant also causes a decrease in the fluorescence quantum yield, from 52% (hexane) to 16% (acetonitrile), probably attributable to the relative increase of non-radiative decay because of the red-shift of the emission.

As observable in Figure 4, the Stokes shift $\tilde{\upsilon}_A$-$\tilde{\upsilon}_F$ increases roughly linearly with the orientation polarizability Δf (Pearson's coefficient R = 0.99), accordingly to the Lippert-Mataga equation (Equation (3)) [50,51]. h is Planck's constant, c is the speed of light in vacuum, a_s is the radius of the cavity in which molecule resides, and μ_e and μ_g are the dipole moments of the excited and ground state, respectively. The plot in Figure 4 confirms that the solvatochromic effect is related to specific solute-solvent interactions that involve the polarization [52].

$$\tilde{\upsilon}_A - \tilde{\upsilon}_F = 2\, h^{-1} c^{-1} (\mu_e - \mu_g)^2\, a_s^{-3}\, \Delta f + \text{constant} \quad (3)$$

The a_s radius obtained from the C-PCM/DFT optimization of the structure of BTD^{NMe2} is 3.92 Å. On the basis of Equation (3), the increase of dipole moment from the ground to the excited state is about 7 D.

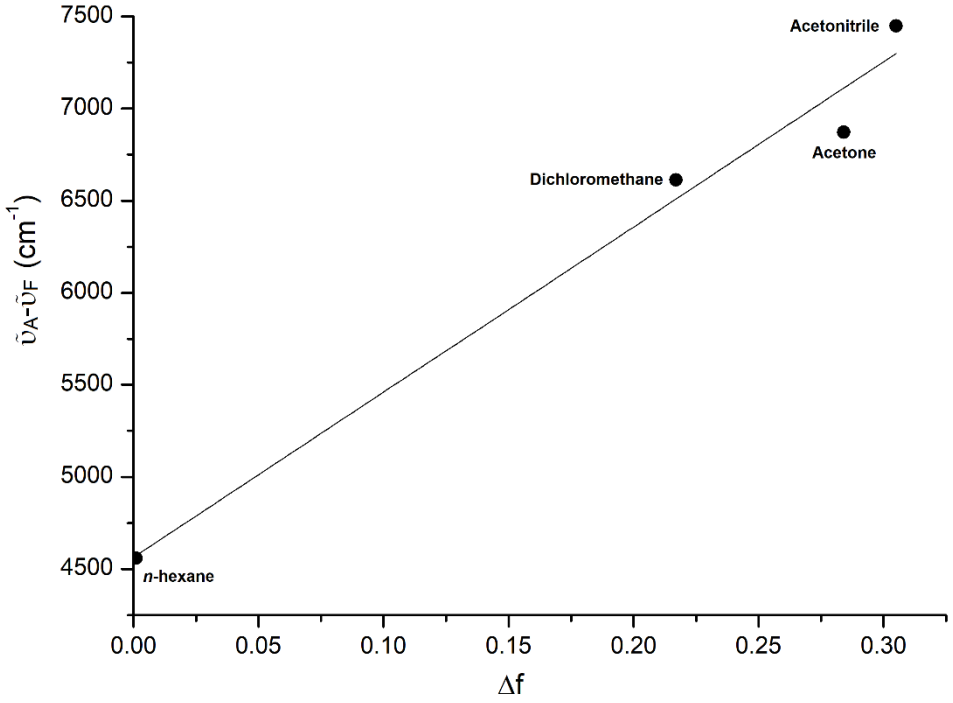

Figure 4. Lippert-Mataga plot.

The luminescent properties of BTD^{NMe2} were maintained after incapsulation in PMMA matrix. The emission falls in the orange region of the CIE diagram with unitary colour purity, as observable in the CIE 1931 chromaticity diagram and in the picture reported as inset in Figure 3.

The photoluminescent properties were justified by means of electrochemical measurements and DFT calculations. As observable from the square wave voltammetries reported in Figure 5, the gap HOMO-LUMO can be estimated around 2.5 eV on considering the irreversible oxidation and reduction processes. Such outcome is in agreement with the onset of the absorption spectrum using acetonitrile as solvent. TD-DFT calculations confirm that the lowest energy transition occurs between HOMO and LUMO, that are π and π* frontier molecular orbitals mostly localized on the benzothiadiazole skeleton, with a contribution in both the molecular orbitals of the *N*,*N*-dimethylamino moiety (Figure 5).

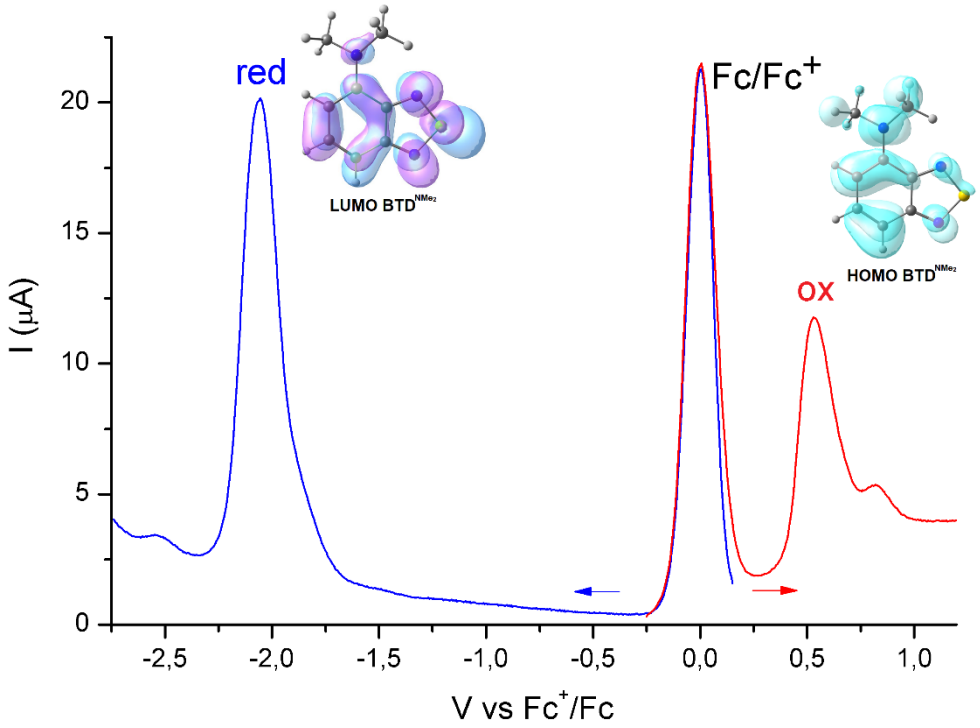

Figure 5. Square wave voltammetry of BTD^{NMe2} ($CH_3CN/LiClO_4$, ferrocene as internal reference, blue line: reduction, red line: oxidation) and frontier molecular orbitals (surface isovalue = 0.03 a.u.).

4. Conclusions

N,N-dimethyl-4-amino-2,1,3-benzothiadiazole (BTD^{NMe2}) was prepared from 2,1,3-benzothiadiazole in a three steps synthetic path that involved nitration, subsequent reduction and methylation. The compound was fully characterized by means of nuclear magnetic resonance (NMR) and infrared spectroscopy. The compound revealed to be highly fluorescent and characterized by a noticeable solvatochromism. The emission features, rationalized on the basis of electrochemical measurements and DFT calculations, were maintained once embedded in poly(methyl methacrylate). The photoluminescence properties exhibited by BTD^{NMe2} make it a suitable candidate for advanced technology applications, and further functionalizations are under current investigation.

Author Contributions: Conceptualization, V.F. and M.B.; methodology, M.B.; software, V.F. and M.B.; validation, M.B.; formal analysis, V.F. and M.B.; investigation, V.F., M.G. and M.B.; resources, M.B.; data curation, V.F. and M.B.; writing—original draft preparation, V.F. and M.B.; writing—review and editing, V.F. and M.B.; visualization, M.B.; supervision, V.F. and M.B.; project administration, M.B.; funding acquisition, M.B. All authors have read and agreed to the published version of the manuscript.

Funding: This research was funded by Università Ca' Foscari Venezia, Bando Spin 2018, D. R. 1065/2018 prot. 67416.

Institutional Review Board Statement: Not applicable.

Informed Consent Statement: Not applicable.

Acknowledgments: Università Ca' Foscari Venezia is gratefully acknowledged for financial support (Bando Spin 2018, D. R. 1065/2018 prot. 67416). We acknowledge CINECA (COLUMN project 2020) for the availability of high performance computing resources.

Conflicts of Interest: The authors declare no conflict of interest.

References

1. Neto, B.A.D.; Lapis, A.A.M.; da Silva Júnior, E.N.; Dupont, J. 2,1,3-benzothiadiazole and derivatives: Synthesis, properties, reactions, and applications in light technology of small molecules. *Eur. J. Org. Chem.* **2013**, *2013*, 228–255, doi:10.1002/ejoc.201201161.
2. Sukhikh, T.S.; Ogienko, D.S.; Bashirov, D.A.; Konchenkoa, S.N. Luminescent complexes of 2,1,3-benzothiadiazole derivatives. *Russ. Chem. Bull.* **2019**, *68*, 651–661, doi:10.1007/s11172-019-2472-9.
3. Langis-Barsetti, S.; Maris, T.; Wuest, J.D. Molecular organization of 2,1,3-benzothiadiazoles in the solid state. *J. Org. Chem.* **2017**, *82*, 5034–5045, doi:10.1021/acs.joc.6b02778.
4. Nakabayashi, K.; Takahashi, T.; Sugawara, R.; Lo, C.-T.; Mori, H. Benzothiadiazole-based donor–acceptor nanoparticles with solvatochromic and thermoresponsive properties. *React. Funct. Polym.* **2018**, *31*, 350–360, doi:10.1016/j.reactfunctpolym.2018.08.011.
5. Benevides, T.O.; Regis, E.; Nicoleti, C.S.; Bechtold, I.H.; Vieira, A.A. Phase-dependent photoluminescence of non-symmetric 2,1,3-benzothiadiazole liquid crystals. *Dyes Pigm.* **2019**, *163*, 300–307, doi:10.1016/j.dyepig.2018.12.012.
6. Zhao, X.; Chaudhry, S.T.; Mei, J. Heterocyclic building blocks for organic semiconductors. *Adv. Heterocycl. Chem.* **2017**, *121*, 133–171, doi:10.1016/bs.aihch.2016.04.009.
7. Volz, D.; Wallesch, M.; Fléchon, C.; Danz, M.; Verma, A.; Navarro, J.M.; Zink, D.M.; Bräse, S.; Baumann, T. From iridium and platinum to copper and carbon: New avenues for more sustainability in organic light-emitting diodes. *Green Chem.* **2017**, *17*, 1988–2011, doi:10.1039/c4gc02195a.
8. Zhang, Y.; Song, J.; Qu, J.; Qian, P.-C.; Wong, W.-Y. Recent progress of electronic materials based on 2,1,3-benzothiadiazole and its derivatives: Synthesis and their application in organic light-emitting diodes. *Sci. China Chem.* **2021**, *64*, 341–357, doi:10.1007/s11426-020-9901-4.
9. Pazini, A.; Maqueira, L.; Stieler, R.; Aucélio, R.Q.; Limberger, J. Synthesis, characterization and photophysical properties of luminescent non-symmetric 4-pyridyl benzothiadiazole derivatives. *J. Mol. Struct.* **2017**, *1131*, 181–189, doi:10.1016/j.molstruc.2016.11.050.
10. Bardi, B.; Dall'Agnese, C.; Moineau-Chane Ching, K.I.; Painelli, A.; Terenziani, F. Spectroscopic investigation and theoretical modeling of benzothiadiazole-based charge-transfer chromophores: From solution to nanoaggregates. *J. Phys. Chem. C* **2017**, *121*, 17466–17478, doi:10.1021/acs.jpcc.7b04647.
11. Pazini, A.; Maqueira, L.; Avila, H.C.; Valente, F.M.; Aderne, R.E.; Back, D.; Aucélio, R.Q.; Cremona, M.; Limberger, J. Phenoxybenzothiadiazole dyes: Synthesis, photophysical properties and preliminary application in OLEDs. *Tetrahedron Lett.* **2018**, *59*, 2994–2999, doi:10.1016/j.tetlet.2018.06.052.
12. Paczkowski, I.M.; Coelho, F.L.; Campo, L.F. 2,1,3-Benzothiadiazole dyes conjugated with benzothiazole and benzoxazole: Synthesis, solvatochromism and solid-state properties. *J. Mol. Liq.* **2020**, *319*, 114277, doi:10.1016/j.molliq.2020.114277.
13. Paisley, N.R.; Tonge, C.M.; Mayder, D.M.; Thompson, K.A.; Hudson, Z.M. Tunable benzothiadiazole-based donor–acceptor materials for two-photon excited fluorescence. *Mater. Chem. Front.* **2020**, *4*, 555—566, doi:10.1039/C9QM00627C.
14. Gao, S.; Balan, B.; Yoosaf, K.; Monti, F.; Bandini, E.; Barbieri, A.; Armaroli, N. Highly efficient luminescent solar concentrators based on benzoheterodiazole dyes with large stokes shifts. *Chem. Eur. J.* **2020**, *26*, 11013—11023, doi:10.1002/chem.202001210.
15. Wu, Y.; Zhu, W. Organic sensitizers from D–π–A to D–A–π–A: Effect of the internal electron-withdrawing units on molecular absorption, energy levels and photovoltaic performances. *Chem. Soc. Rev.* **2013**, *42*, 2039—2058, doi:10.1039/c2cs35346f.
16. Holliday, S.; Li, Y.; Luscombe, C.K. Recent advances in high performance donor-acceptor polymers for organic photovoltaics. *Prog. Polym. Sci.* **2017**, *70*, 34–51, doi:10.1016/j.progpolymsci.2017.03.003.
17. Zheng, P.; Xu, J.; Peng, F.; Peng, S.; Liao, J.; Zhao, H.; Li, L.; Zeng, X.; Yu, H. Novel dual acceptor (D–D′–A′–π–A) dye-sensitized solar cells based on the triarylamine structure and benzothiadiazole double electron withdrawing unit. *New J. Chem.* **2021**, *45*, 4443–4452, doi: 10.1039/d0nj05319h.
18. Wang, C.; Liu, F.; Chen, Q.-M.; Xiao, C.-Y.; Wu, Y.-G.; Li, W.-W. Benzothiadiazole-based conjugated polymers for organic solar cells. *Chin. J. Polym. Sci.* **2021**, *39*, 525–536, doi: 10.1007/s10118-021-2537-8.
19. Raitz, I.; de Souza Filho, R.Y.; de Andrade, L.P.; Correa, J.R.; Neto, B.A.D.; Pilli, R.A. Preferential mitochondrial localization of a goniothalamin fluorescent derivative. *ACS Omega* **2017**, *2*, 3774–3784, doi:10.1021/acsomega.7b00416.
20. Appelqvist, H.; Stranius, K.; Börjesson, K.; Nilsson, K.P.R.; Dyrager, C. Specific imaging of intracellular lipid droplets using a benzothiadiazole derivative with solvatochromic properties. *Bioconjugate Chem.* **2017**, *28*, 1363–1370, doi:10.1021/acs.bioconjchem.7b00048.
21. Souza, V.S.; Corrêa, J.R.; Carvalho, P.H.P.R.; Zanotto, G.M.; Matiello, G.I.; Guido, B.C.; Gatto, C.C.; Ebeling, G.; Gonçalves, P.F.B.; Dupont, J.; et al. Appending ionic liquids to fluorescent benzothiadiazole derivatives: Light up and selective lysosome staining. *Sens. Actuators B Chem.* **2020**, *321*, 128530, doi:10.1016/j.snb.2020.128530.
22. Uchiyama, S.; Tsuji, T.; Ikado, K.; Yoshida, A.; Kawamoto, K.; Hayashic, T.; Inadac, N. A cationic fluorescent polymeric thermometer for the ratiometric sensing of intracellular temperature. *Analyst* **2015**, *140*, 4498–4506, doi:10.1039/c5an00420a.
23. Uchiyama, S.; Kimura, K.; Gota, C.; Okabe, K.; Kawamoto, K.; Inada, N.; Yoshihara, T.; Tobita, S. Environment-sensitive fluorophores with benzothiadiazole and benzoselenadiazole structures as candidate components of a fluorescent polymeric thermometer. *Chem. Eur. J.* **2012**, *18*, 9552–9563, doi:10.1002/chem.201200597.

24. Li, R.; Byun, J.; Huang, W.; Ayed, C.; Wang, L.; Zhang, K.A.I. Poly(benzothiadiazoles) and their derivatives as heterogeneous photocatalysts for visible-light-driven chemical transformations. *ACS Catal.* **2018**, *8*, 4735–4750, doi:10.1021/acscatal.8b00407.
25. Wang, G.-B.; Li, S.; Yan, C.-X.; Lin, Q.-Q.; Zhu, F.-C.; Geng, Y.; Dong, Y.-B. A benzothiadiazole-based covalent organic framework for highly efficient visible-light driven hydrogen evolution. *Chem. Commun.* **2020**, *56*, 12612–12615, doi:10.1039/d0cc05222a.
26. Broncová, G.; Shishkanova, T.V.; Dendisová, M.; Člupek, M.; Kubáč, D.; Matějka, P. Poly(4-amino-2,1,3-benzothiadiazole) films: Preparation, characterization and applications. *Chem. Pap.* **2017**, *71*, 359–366, doi:10.1007/s11696-016-0045-z.
27. Munakata, M.; He, H.; Kuroda-Sowa, T.; Maekawa, M.; Suenaga, Y. Dicopper complexes derived from 4-amino-2,1,3-benzothiadiazole with versatile co-ordination number and geometry. *J. Chem. Soc., Dalton Trans.* **1998**, 1499–1502, doi:10.1039/A800549D.
28. Bashirov, D.A.; Sukhikh, T.S.; Kuratieva, N.V.; Chulanova, E.A.; Yushina, I.V.; Gritsan, N.P.; Konchenko, S.N.; Zibarev, A.V.; Novel applications of functionalized 2,1,3-benzothiadiazoles for coordination chemistry and crystal engineering. *RSC Adv.* **2014**, *4*, 28309–28316, doi:10.1039/C4RA03342F.
29. Sukhikh, T.S.; Ogienko, D.S.; Bashirov, D.A.; Kuratieva, N.V.; Komarov, V.Yu.; Rakhmanova, M.I.; Konchenko, S.N. New red-luminescent cadmium coordination polymers with 4-amino-2,1,3-benzothiadiazole. *J. Coord. Chem.* **2016**, *69*, 3284–3293, doi:10.1080/00958972.2016.1231304.
30. Sukhikh, T.S.; Bashirov, D.A.; Ogienko, D.S.; Kuratieva, N.V.; Sherin, P.S.; Rakhmanova, M.I.; Chulanova, E.A.; Gritsan, N.P.; Konchenko, S.N.; Zibarev, A.V. Novel luminescent β-ketoimine derivative of 2,1,3-benzothiadiazole: Synthesis, complexation with Zn(ii) and photophysical properties in comparison with related compounds. *RSC Adv.* **2016**, *6*, 43901–43910, doi:10.1039/c6ra06547c.
31. Sukhikh, T.S.; Komarov, V.Yu.; Konchenko, S.N.; Benassi, E. The hows and whys of peculiar coordination of 4-amino-2,1,3-benzothiadiazole. *Polyhedron* **2018**, *139*, 33–43, doi:10.1016/j.poly.2017.09.048.
32. Sukhikh, T.S.; Bashirov, D.A.; Shuvaev, S.; Komarov, V.Yu.; Kuratieva, N.V.; Konchenko, S.N.; Benassi, E. Noncovalent interactions and photophysical properties of new Ag(I) complexes with 4-amino-2,1,3-benzothiadiazole. *Polyhedron* **2018**, *141*, 77–86, doi:10.1016/j.poly.2017.11.017.
33. Sukhikh, T.S.; Khisamov, R.M.; Bashirov, D.A.; Komarov, V.Y.; Molokeev, M.S.; Ryadun, A.A.; Benassi, E.; Konchenko, S.N. Tuning of the coordination and emission properties of 4-amino-2,1,3-benzothiadiazole by introduction of diphenylphosphine group. *Cryst. Growth Des.* **2020**, *20*, 5796–5807, doi:10.1021/acs.cgd.0c00406.
34. Slavachevskaya, N.M.; Belen'kaya, I.A.; Tsepova, N.S.; Levocheskaya, E.I.; Krasil'nikov, I.I. Synthesis of certain quaternary derivatives in the aminophenol and benzo-2,1,3-thiadiazole series as potential radiation-protecting materials. *Pharm. Chem. J.* **1976**, *10*, 327–331, doi:10.1007/BF00757982.
35. Armarego, W.L.F.; Perrin, D.D. *Purification of Laboratory Chemicals*, 4th ed.; Butterworth-Heinemann: Oxford, UK, 1996.
36. Komin, A.P.; Carmack, M. The chemistry of 1,2,5-thiadiazoles, IV. Benzo [1,2-c:3,4-c':5,6-c"] tris [1,2,5] thiadiazole. *J. Heterocycl. Chem.* **1975**, *12*, 829–833, doi:10.1002/jhet.5570120503.
37. da Silva Miranda, F.; Signori, A.M.; Vicente, J.; de Souza, B.; Priebe, J.P.; Szpoganicz, B.; Sanches Gonçalves, N.; Neves, A. Synthesis of substituted dipyrido[3,2-a:2′,3′-c]phenazines and a new heterocyclic dipyrido[3,2-f:2′,3′-h]quinoxalino[2,3-b]quinoxaline. *Tetrahedron* **2008**, *64*, 5410–5415, doi:10.1016/j.tet.2008.02.097.
38. Liu, Y.; Lu, Y.; Prashad, M.; Repič, O.; Blacklock, T.J. A practical and chemoselective reduction of nitroarenes to anilines using activated iron. *Adv. Synth. Catal.* **2005**, *347*, 217–219, doi:10.1002/adsc.200404236.
39. Fery-Forgues, S.; Lavabre, D. Are fluorescence quantum yields so tricky to measure? a demonstration using familiar stationery products. *J. Chem. Educ.* **1999**, *76*, 1260–1264, doi:10.1021/ed076p1260.
40. Gerber, I.C.; Ángyán, J.G. Hybrid functional with separated range. *Chem. Phys. Lett.* **2005**, *415*, 100–105, doi:10.1016/j.cplett.2005.08.060.
41. Chai, J.D.; Head-Gordon, M. Long-range corrected hybrid density functionals with damped atom–atom dispersion corrections. *Phys. Chem. Chem. Phys.* **2008**, *10*, 6615–6620, doi:10.1039/B810189B.
42. Minenkov, Y.; Singstad, Å.; Occhipinti, G.; Jensen, V.R. The accuracy of DFT-optimized geometries of functional transition metal compounds: A validation study of catalysts for olefin metathesis and other reactions in the homogeneous phase. *Dalton Trans.* **2012**, *41*, 5526–5541, doi:10.1039/C2DT12232D.
43. Weigend, F.; Ahlrichs, R. Balanced basis sets of split valence, triple zeta valence and quadruple zeta valence quality for H to Rn: Design and assessment of accuracy. *Phys. Chem. Chem. Phys.* **2005**, *7*, 3297–3305, doi:10.1039/B508541A.
44. Cossi, M.; Rega, N.; Scalmani, G.; Barone, V. Energies, structures, and electronic properties of molecules in solution with the CPCM solvation model. *J. Comput. Chem.* **2003**, *24*, 669–681, doi:10.1002/jcc.10189.
45. Barone, V.; Cossi, M. Quantum calculation of molecular energies and energy gradients in solution by a conductor solven-model. *J. Phys. Chem. A* **1998**, *102*, 1995–2001, doi:10.1021/jp9716997.
46. Ullrich, C.A. *Time-Dependent Density Functional Theory*; Oxford University Press: Oxford, UK, 2012.
47. Frisch, M.J.; Trucks, G.W.; Schlegel, H.B.; Scuseria, G.E.; Robb, M.A.; Cheeseman, J.R.; Scalmani, G.; Barone, V.; Petersson, G.A.; Nakatsuji, H.; et al. *Gaussian 16, Revision C.01*; Gaussian, Inc.: Wallingford, CT, USA, 2016.
48. Reddy, M.D.; Fronczek, F.R., Watkins, E.B. Rh-catalyzed, regioselective, C–H bond functionalization: Access to quinoline-branched amines and dimers. *Org. Lett.* **2016**, *18*, 5620–5623, doi:10.1021/acs.orglett.6b02848.
49. Eaton, D.F. Reference materials for fluorescence measurement. *Pure Appl. Chem.* **1988**, *60*, 1107–1114, doi:10.1351/pac198860071107.

50. Valeur, B. *Molecular Fluorescence: Principles and Applications*; WILEY-VCH Verlag GmbH: Weinheim, Germany, 2002.
51. Mataga, N.; Kaifu, Y.; Koizumi, M. Solvent effects upon fluorescence spectra and the dipole moments of excited molecules. *Bull. Chem. Soc. Jpn.* **1956**, *29*, 465–470, doi:10.1246/bcsj.29.465.
52. Lakowicz, J.R. *Principles of Fluorescence Spectroscopy*, 3rd ed.; Springer: Singapore; Japan, 2006.